COMPARATIVE ANALYSIS OF THE PLANE COUETTE FLOW OF COUPLE STRESS FLUID UNDER THE INFLUENCE OF MAGNETOHYDRODYNAMICS

Muhammad Farooq[a], Ibrar Khan[a], Rashid Nawaz[b], Gamal M. Ismail[c,*], Huzaifa Umar[d], Hijaz Ahmad[d,c,e]

[a] Department of Mathematics, Abdul Wali Khan University, Mardan 23200, Pakistan
[b] UniSa STEM, University of South Australia
[c] Department of Mathematics, Faculty of Science, Islamic University of Madinah, Madinah, Saudi Arabia
[d] Near East University, Operational Research Center in Healthcare,
Near East Boulevard, PC: 99138 Nicosia/Mersin 10, Turkey
[e] Department of Mathematics and Informatics, Azerbaijan University,
Jeyhun Hajibeyli street, 71, AZ1007, Baku, Azerbaijan
*Corresponding Author e-mail: gismail@iu.edu.sa

The present study aims to perform a comparative analysis of the plane Couette flow of a couple stress fluid under the influence of magnetohydrodynamics (MHD) using two different methods: the Optimal Auxiliary Function Method (OAFM) and the Homotopy Perturbation Method (HPM). The couple stress fluid is known for its non-Newtonian behavior, where the fluid's response to shear is influenced by the presence of internal microstructure.The OAFM and HPM are utlized to solve the governing equations of the couple stress fluid flow under MHD. The OAFM is a numerical technique that involves introducing an auxiliary function to simplify the equations, leading to an easier solution procedure. On the other hand, HPM is an analytical method that employs a series solution .The comparative analysis focuses on examining the accuracy, efficiency, and convergence behavior of the two methods. Various flow parameters such as the couple stress parameter, the magnetic parameter, and the velocity ratio are considered to investigate their influence on the flow behavior. Furthermore the HPM solution was compared with the OAFM solution using different graphs and tables.It reveals that the solution obtained by HPM is batter than OAFM solution.

Keywords: *Couple stress fluid; Optimal Auxiliary Function Method (OAFM); Homotopy Perturbation Method (HPM); magnetohydrodynamics (MHD)*

PACS: specify the PACS code(s) here

1. INTRODUCTION

In recent years, the magnetohydrodynamic (MHD) flow and heat transfer have obtained a wide concern, because of its various applications, such as nuclear reactor, physics, ocean dynamics, the generation of MHD energy [1, 2], chemical manufacturing, and the synthesis of magnetic liquids [3, 4, ?, 7, 8, 9, 10, 11]. Ahmed et al. [12] conducted a theoretical study of an electrically conducting couple stress fluid (CSF) in an oscillatory viscous flow with heat transfer influenced by convection and MHD, which has important applications in the production of electro-conductive polymers and liquids. Ajaz [13] investigated the influence of an applied inclined magnetic field on the peristaltic flow that occurs during heat and mass transfer in a CSF. Pei-Ying and colleagues [14] evaluated the velocity and temperature distributions of hafnium nanoparticles subjected to a thermal radiation effect and a magnetic field. They do this by compiling the findings of varying thermal conductivity and viscosity in the hafnium nanoparticles' appearance. Ajala et al. [15] studied how the existence of a variable viscosity and thermal radiation affects the flow of a two-dimensional boundary layer. Falade et al. [16] investigated the minimization of the entropy generation rate as a result of temperature-dependent viscosity and couple stress fluid caused by the heated channel. This is done to lower the entropy production rate to its lowest attainable value. Swarnalathamma et al. [17] and Ramesh [18] studied the influence of heat transfer on the peristaltic flow of a couple stress fluid with MHD and a porous media. They looked at how the new factors affected the peristaltic pumping rate, frictional forces, velocity, temperature, pressure gradient, and concentration fields. Divya et al. [19] reported and analysed the combined impact of temperature-dependent viscosity and thermal conductivity on the MHD peristaltic flow of the Bingham fluid in a porous medium with heat transfer. This is done in order to better understand how these factors affect the flow of the Bingham fluid. The authors analysed

the effects of these variables on temperature as well as pumping rate and heat transfer coefficient. In their study of an unsteady three-dimensional flow over a stretched surface accompanied by a chemical reaction, Hayat et al. [20] came to the conclusion that both the velocity field and the associated boundary layer thickness decreased as a function of the couple stress parameter. This is one of the findings of their study.

In this paper, the couette flow of couple stress fluids between two parallel plates under the influence of MHD has been explored utilising the two well known approaches the Homotopy Perturbation Method (HPM)[21],[22] and the Optimal Auxiliary Function Method (OAFM)[23],[24]. Results obtained by the proposed approaches are compared with each other using various graphs and tables. The residual error obtained using the proposed methods reveals the HPM solution is better than the OAFM solution. Graphs have been utilised to demonstrate how the non-dimensional parameters affect the flow pattern.

The rest of the paper is organized as: Section (2) provides general methodology of the HPM and OAFM. Section (3) contains basic equation of couple stress fluid and problem formulation. Solution of the problem is provided in section (4). Section (5) discusses the numerical results and discussion. Section (6) provides final conclusion.

2. GENERAL METHODOLOGY OF THE PROPOSED METHODS
2.1. Homotopy Perturbation Method

To explain the general idea of the homotopy perturbation method, we consider the nonlinear differential equation illustrated below.

$$N(u(y)) - \eta(r) = 0, \quad r \in \Omega, \tag{1}$$

$$B(u, \frac{\partial u}{\partial y}), \ r \in \Omega, \tag{2}$$

where N is the combination of the linear $\psi(u)$ and nonlinear $\aleph(u)$, differential operators and B represents boundary conditions, $\eta(r)$ is the known analytical function. Therefore Eq.(1) can be written as:

$$\psi(u) + \aleph(u) - \eta(r) = 0. \tag{3}$$

We construct mapping for homotopy:

$$H(u, \rho) : \Omega \times [0, 1] \to R, \tag{4}$$

$$H(u, \rho) = (1 - \rho)[\psi(u) - \psi(u_0)] + \rho[\psi(u) + \aleph(u) - \eta(r)] = 0, \tag{5}$$

$$u(y, \rho) : \Omega \times [0, 1] \to R, \tag{6}$$

where ρ is the homotopy parameter and when $\rho = 0$, then u_0 is the initial approximation that satisfies boundary conditions. When $\rho = 1$, the solution can be written in the form

$$u = u_0 + \rho u_1 + \rho^2 u_2 + \rho^3 u_3 + ... \tag{7}$$

Homotopy perturbation method is the combine process of homotopy and perturbation.

2.2. Analysis of Optimal Axillary Functions Method

To explore the general procedure of the optimal axillary functions method, we consider the nonlinear differential equation illustrated below.

$$L(u) + N(u) + h(y) = 0. \tag{8}$$

the associated boundary condition are:

$$B(u(y), \frac{\partial u(y)}{\partial y}) = 0. \tag{9}$$

In Eq.(8) L is linear , N denotes the non-linear differential operator and $h(y)$ is the known function. The approximate solution of Eq.(8) can be written as

$$u^*(y, C_i) = u_0(y) + u_1(y, C_n), \quad n = 1, 2, 3, 4...s. \tag{10}$$

where C_n are the auxiliary constant. To fined the initial and first approximate solution of Eq.(8) we use Eq.(10) in Eq.(8), which reveals

$$L(u_0(y) + y_1(y, C_n)) + N(u_0(y) + u_1(y, C_n)) + h(y) = 0. \tag{11}$$

For obtaining the initial approximation $u_0(y)$, we use the following linear equation.

$$L(u_0(y)) + h(y) = 0, \quad B(u_0, \frac{du_0}{y}) = 0. \tag{12}$$

The first-order approximation $u_1(y)$ can be found from the following equation:

$$L(u_1(y, C_n)) + N(u_0(y) + u_1(y, C_n)) = 0, \tag{13}$$

with associated boundary condition:

$$B(u_1(y, C_n), \frac{\partial u_1(y, C_n)}{\partial y}) = 0. \tag{14}$$

The non-linear tern from equation (13) can be expanded in the form

$$N(u_0(y) + u_1(y, C_n)) = N(u_0(y)) + \sum_{k=1}^{\infty} \frac{u_1^{(k)}(y, C_n)}{k!} N^{(k)}(u_0(y)). \tag{15}$$

Equation (15) can be stated in the algorithmic sequence to achieve the limit solution. To control all the challenges that are occur while solving the non-linear differential of Eq.(11) and to accelerate the convergence of the first approximation $u_1(y, C_n)$. We use an alternate expression which represent the Eq.(13)

$$L(u_1(y, C_n)) + A_1(u_0(y), C_n)N(u_0(y)))) + A_2(u_0(y), C_m) = 0, \tag{16}$$

$$B(u_1(y, C_n), \frac{du_1(y, C_n)}{dy}) = 0, \tag{17}$$

Remark 1. A_1 and A_2 are assumed to be two axillary functions which depend on the $u_0(y)$ and unknown C_n and C_m parameters where $n = 1, 2, 3, ...s$ and $m = s + 1, s + 2, s + 3...q$.

Remark 2.

A_1 and A_2 are not fixed. It may be $u_0(y)$ or $N(u_0(y))$ and can be the combination of both $u_0(y)$ and $N(u_0(y))$.

Remark 3. The auxiliary constants C_n and C_m can be determined using different methods either by Collocation method, Least square method or Galerkin's method.

3. BASIC EQUATIONS AND PROBLEM FORMULATION

The basic equations for an incompressible couple stress fluid are as follows [25],[26]:

$$\nabla.\mathbf{V} = 0 \tag{18}$$

$$\rho(\frac{\partial}{\partial t} + \mathbf{V}.\nabla)\mathbf{V} = \nabla.\mathbf{S} - \eta\nabla^4\mathbf{V} + \rho f + \mathbf{J} \times \mathbf{B} \tag{19}$$

$$\rho C_p(\frac{\partial}{\partial t} + \mathbf{V}.\nabla)\Theta = \kappa\nabla^2\Theta + tr(\mathbf{S}.L) \tag{20}$$

Where the velocity vector is symbolized by $\mathbf{V}$, the body force per unit mass is f, the constant density is denoted as ρ, $\mathbf{S}$ is the Cauchy stress tensor, Θ is the temperature, κ is the thermal conductivity,$\mathbf{J}$ represents current density, $\mathbf{B}$ represents magnetic induction ,C_p symbolizes the specific heat, also the gradient of $\mathbf{V}$ is denoted by L, and η is used for couple stress parameter. The material derivative is indicated by $\frac{D}{Dt}$ and is defined by the following:

$$\frac{D(*)}{Dt} = (\frac{\partial}{\partial t} + \mathbf{V}.\nabla)(*) \tag{21}$$

The Cauchy stress tensor is represented and defined as

$$\mathbf{S} = -pI + \mu A_1 \tag{22}$$

Where I represent the unit tensor, p indicates the dynamic pressure and μ is the viscosity constant. The first Rivilin-Ericksen tensor is defined and represented as

$$A_1 = L + L^t, \tag{23}$$

where L^t is the transpose of L.

3.1. Problem Formulation

Consider the Couette flow of a couple stress fluid under the influence of MHD between two infinite parallel plates separated by 2d, where the upper plate moves with constant velocity U and the lower plate remains stationary (Figure 1). 1. The temperature of the lower upper and plates are Θ_0 and Θ_1 respectively. Both plates are situated in the plane at $y = -d$ and $y = d$ in an orthogonal coordinate system (x, y), where the fluid is moving in the x-axis direction and the y-axis is perpendicular to the plates.Here, the viscosity is assumed to be a function of temperature $\Theta(y)$, the pressure gradient is set to zero, and the velocity and temperature fields are chosen as follows:

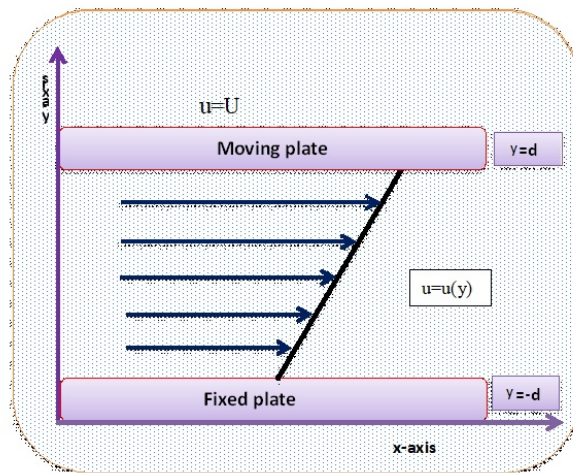$$\mathbf{V} = [u(y), 0, 0], \quad \Theta = \Theta(y) \tag{24}$$

Figure 1. Geometry of the problem

These assumptions lead us to the conclusion that the continuity Eq.(18) is identically satisfied and the momentum Eq.(19) simplifies to

$$0 = -\frac{\partial p}{\partial x} + \frac{\partial \mathbf{S}_{xx}}{\partial x} + \frac{\partial \mathbf{S}_{xy}}{\partial y} + \frac{\partial \mathbf{S}_{xz}}{\partial z} - \eta \frac{d^4 u}{d^4 y} - \sigma B_0^2 u, \tag{25}$$

$$0 = -\frac{\partial p}{\partial y} + \frac{\partial \mathbf{S}_{yx}}{\partial x} + \frac{\partial \mathbf{S}_{yy}}{\partial y} + \frac{\partial \mathbf{S}_{yz}}{\partial z}, \tag{26}$$

$$0 = -\frac{\partial p}{\partial z} + \frac{\partial \mathbf{S}_{zx}}{\partial x} + \frac{\partial \mathbf{S}_{zy}}{\partial y} + \frac{\partial \mathbf{S}_{zz}}{\partial z}. \tag{27}$$

Where B_0 represents the applied magnetic field and σ denotes electric conductivity of the fluid.
We have

$$\mathbf{S}_{xx} = \mathbf{S}_{yy} = \mathbf{S}_{zz} = \mathbf{S}_{yz} = \mathbf{S}_{zy} = \mathbf{S}_{xz} = \mathbf{S}_{zx} = 0, \quad \mathbf{S}_{xy} = \mathbf{S}_{yx} = \mu \frac{du}{dy}. \tag{28}$$

Obtaining the velocity profile using equation Eq.(25). This equation may also be stated as

$$\eta \frac{d^4 u}{dy^4} - \mu \frac{d^2 u}{dy^2} - \frac{d\mu}{dy} \frac{du}{dy} + \sigma B_0^2 u = 0. \tag{29}$$

After all assumptions are applied, the energy equation (20) simplifies to Eq. (30).

$$\frac{d^2 \Theta}{dy^2} + \frac{\mu}{\kappa} (\frac{du}{dy})^2 + \frac{\mu}{\kappa} (\frac{d^2 u}{dy^2})^2 = 0. \tag{30}$$

The associated boundary condition are

$$u(-d) = 0, \quad u(d) = U, \tag{31}$$

$$u''(-d) = 0, \quad u''(-d) = 0, \tag{32}$$

$$\Theta(-d) = \Theta_0, \quad \Theta(d) = \Theta_1. \tag{33}$$

According to Eq. (32), the couple stresses at the plates are zero. We utilize the non-dimensional parameters mentioned below:

$$y^* = \frac{y}{d}, \quad u^* = \frac{u}{U}, \quad \mu^* = \frac{\mu}{\mu_0}, \quad \Theta^* = \frac{\Theta - \Theta_0}{\Theta_0 - \Theta_1},$$

$$\beta^2 = \frac{d^2 \mu_0}{\eta}, \quad R = \frac{\sigma d^4 B_0^2}{\eta}, \quad \lambda = \frac{\mu_0 U^2}{\kappa(\Theta_0 - \Theta_1)}$$

Where λ is the Brinkman number, μ is the reference viscosity, and U is the reference velocity. Using these dimensionless parameters, Eqs.(29) and (30) along with the boundary conditions becomes.

$$\frac{d^4 u}{dy^4} - \beta^2 \mu \frac{d^2 u}{dy^2} - \beta^2 \frac{d\mu}{dy} \frac{du}{dy} + Ru = 0, u(-1) = 0, \quad u(1) = 1, \quad u''(-1) = 0, \quad u''(-1) = 0. \tag{34}$$

$$\frac{d^2 \Theta}{dy^2} + \lambda \mu (\frac{du}{dy})^2 + \frac{\lambda}{\beta^2} (\frac{d^2 u}{dy^2})^2 = 0, \quad \Theta(-1) = 0, \quad \Theta(1) = 1. \tag{35}$$

The dimensionless form of the Reynolds viscosity is expressed as follows [27, 28, 29].

$$\mu = e^{-M\Theta} \tag{36}$$

Using Taylor series expansion to Eq. (36) we get

$$\mu = 1 - M\Theta, \quad \frac{d\mu}{dy} = -M \frac{d\Theta}{dy} \tag{37}$$

The coupled system illustrated below is created by replacing Eq. (37) in the governing Eqs. (34) and (35), respectively:

$$\frac{d^4 u}{dy^4} - \beta^2 (1 - M\Theta) \frac{d^2 u}{dy^2} + \beta^2 M \frac{d\Theta}{dy} \frac{du}{dy} + Ru = 0, \tag{38}$$

$$u(-1) = 0, \quad u(1) = 1, \quad u''(-1) = 0, \quad u''(-1) = 0,$$

$$\frac{d^2 \Theta}{dy^2} + \lambda(1 - M\Theta)(\frac{du}{dy})^2 + \frac{\lambda}{\beta^2} (\frac{d^2 u}{dy^2})^2 = 0, \quad \Theta(-1) = 0, \quad \Theta(1) = 1. \tag{39}$$

4. SOLUTION OF THE PROBLEM
4.1. HPM Solution

Zeroth order problem.

$$\frac{d^4 u}{dy^4} = 0, \tag{40}$$

$$u(-1) = 0, \quad u(1) = 1, \quad u''(-1) = 0, \quad u''(1) = 0,$$

$$\frac{d^2 \Theta}{dy^2} = 0, \tag{41}$$

$$\Theta(-1) = 0, \quad \Theta(1) = 1.$$

Solution of zeroth order problem

$$u_0(y) = \frac{1+y}{2}, \tag{42}$$

$$\Theta_0(y) = \frac{1+y}{2}. \tag{43}$$

First order problem

$$\frac{d^4 u_1}{dy^4} + \left(\beta^2 M\Theta_0 - \beta^2\right)\frac{d^2 u_0}{dy^2} + \beta^2 M\frac{d\Theta_0}{dy}\frac{du_0}{dy} + Ru_0 = 0 \tag{44}$$

$$u_1(-1) = 0, \quad u_1(1) = 0, \quad u_1''(-1) = 0, \quad u_1''(1) = 0,$$

$$\frac{d^2\Theta_1}{dy^2} + \frac{\lambda}{\beta^2}\left(\frac{d^2 u_0}{dy^2}\right)^2 + (\lambda - M\lambda\Theta_0)\left(\frac{du_0}{dy}\right)^2 = 0, \tag{45}$$

$$\Theta_1(-1) = 0, \quad \Theta_0(1) = 0.$$

Solution of the first order problem.

$$u_1(y) = \frac{1}{1440}\Big(-75\beta^2 M + 90\beta^2 My^2 - 15\beta^2 My^4 - 150R - 14yR + 180y^2R +$$
$$20y^3R - 30y^4R - 6y^5R\Big), \tag{46}$$

$$\Theta_1(y) = \frac{1}{2}(6\lambda - 3M\lambda - My\lambda - 6y^2\lambda + 3My^2\lambda + My^3\lambda). \tag{47}$$

First order HPM solution for velocity profile and temperature distribution are

$$u(y) = u_0(y) + u_1(y) \tag{48}$$

$$\Theta(y) = \Theta_0(y) + \Theta_1(y) \tag{49}$$

$$u(y) = \frac{1+y}{2} + \frac{1}{1440}\Big(-75\beta^2 M + 90\beta^2 My^2 - 15\beta^2 My^4 - 150\gamma - 14yR + 180y^2R +$$
$$20y^3R - 30y^4R - 6y^5R\Big), \tag{50}$$

$$\Theta(y) = \frac{1+y}{2} + \frac{1}{2}(6\lambda - 3M\lambda - My\lambda - 6y^2\lambda + 3My^2\lambda + My^3\lambda). \tag{51}$$

4.2. OAFM Solution

Zeroth component for velocity and temperature distribution.

$$\frac{d^4 u_0}{dy^4} = 0, \tag{52}$$

$$u_0(-1) = 0, \quad u_0(1) = 1, \quad u_0''(-1) = 0, \quad u_0''(1) = 0,$$

$$\frac{d^2\Theta_0}{dy^2} = 0, \tag{53}$$

$$\Theta_0(-1) = 0, \quad \Theta_1(1) = 0.$$

Their solution are

$$u_0(y) = \frac{1+y}{2}, \tag{54}$$

$$\Theta_0(y) = \frac{1+y}{2} \tag{55}$$

consider non Linear term from Eq. (38) and (39)

$$N(u) = -\beta^2(1 - M\Theta)\frac{d^2 u}{dy^2} + \beta^2 M\frac{du}{dy}\frac{d\Theta}{dy} + Ru, \tag{56}$$

$$N(\Theta) = \lambda(1 - M\Theta)\left(\frac{du}{dy}\right)^2 + \frac{\lambda}{\beta^2}\left(\frac{d^2 u}{dy^2}\right)^2. \tag{57}$$

Replace u by u_0 and Θ by Θ_0

$$N(u_0) = -\beta^2(1 - M\Theta_0)\frac{d^2 u_0}{dy^2} + \beta^2 M\frac{du_0}{dy}\frac{d\Theta_0}{dy} + Ru_0, \tag{58}$$

$$N(\Theta_0) = \lambda(1 - M\Theta_0)(\frac{du_0}{dy})^2 + \frac{\lambda}{\beta^2}(\frac{d^2u_0}{dy^2})^2. \tag{59}$$

We are free to choose auxiliary function.

$$A_1 = c1(\frac{1+y}{2})^2, \quad A_2 = c2(\frac{1+y}{2})^3,$$
$$A_3 = c3(\frac{1+y}{2})^5, \quad A_4 = c4(\frac{1+y}{2})^7. \tag{60}$$

Now using Eq.(54), Eq.(55) and Eq.(60) into Eq.(58) and Eq.(59), the nonlinear terms becomes

$$N(u_0) = \frac{\beta^2 M}{4} + \frac{1}{2}R(y+1), \tag{61}$$

$$N(\Theta_0) = \frac{1}{4}\lambda\big(1 - \frac{1}{2}M(y+1)\big). \tag{62}$$

First order approximation can be obtained by

$$\frac{d^4u_1}{dy^4} + A_1N[u_0] + A_2 = 0, \tag{63}$$

$$\frac{d^2\Theta_1}{dy^2} + A_3N[\Theta_0] + A_4 = 0. \tag{64}$$

After applying inverse operator on Eq.(63) and Eq.(64), we get the first order approximation.

$$\begin{aligned}
u_1(y) = \frac{1}{20160}\big(&- 21\beta^2 c_1 M y^5 - 105B^2 c_1 M y^4 + 70B^2 c_1 M y^3 + 630B^2 c_1 M y^2 \\
&- 49\beta^2 c_1 M y - 525\beta^2 c_1 M - 1246c_1 R - 3c_2 y^7 - 14c_1 R y^6 - 21c_2 y^6 \\
&- 84c_1 R y^5 - 63c_2 y^5 - 210c_1 R y^4 - 105c_2 y^4 + 280c_1 R y^3 + 231c_2 y^3 \\
&+ 1470c_1 R y^2 + 945c_2 y^2 - 196c_1 R y - 165c_2 y - 819c_2\big),
\end{aligned} \tag{65}$$

$$\begin{aligned}
\Theta_1(y) = \frac{1}{129024}\big(&9c_3 M y^8\lambda + 72c_3 M y^7\lambda + 252c_3 M y^6\lambda + 504c_4 M y^5\lambda + 630c_3 M y^4\lambda \\
&+ 504c_3 M y^3\lambda + 252c_3 M y^2\lambda - 1080c_3 M y\lambda - 1143c_3 M\lambda - 24c_3 y^7\lambda - \\
&168c_3 y^6\lambda - 504c_3 y^5\lambda - 840c_3 y^4\lambda - 840c_3 y^3\lambda - 504c_3 y^2\lambda + 1368c_3 y\lambda + \\
&1512c_3\lambda - 14c_4 y^9 - 126c_4 y^8 - 504c_4 y^7 - 1176c_4 y^6 - 1764c_4 y^5 - \\
&1764c_4 y^4 - 1176c_4 y^3 - 504c_4 y^2 + 3458c_4 y + 3570c_4\big).
\end{aligned} \tag{66}$$

According to OAFM Procedure.
$$u(y) = u_0(y) + u_1(y) \tag{67}$$

$$\Theta(y) = \Theta_0(y) + \Theta_1(y) \tag{68}$$

$$\begin{aligned}
u(y) = \frac{1+y}{2} + \frac{1}{20160}\big(&- 21\beta^2 c_1 M y^5 - 105B^2 c_1 M y^4 + 70B^2 c_1 M y^3 + 630B^2 c_1 M y^2 \\
&- 49\beta^2 c_1 M y - 525\beta^2 c_1 M - 1246c_1 R - 3c_2 y^7 - 14c_1 R y^6 - 21c_2 y^6 - 84c_1 R y^5 \\
&- 63c_2 y^5 - 210c_1 R y^4 - 105c_2 y^4 + 280c_1 R y^3 + 231c_2 y^3 + 1470c_1 R y^2 + 945c_2 y^2 \\
&- 196c_1 R y - 165c_2 y - 819c_2\big),
\end{aligned} \tag{69}$$

$$\begin{aligned}
\Theta(y) = \frac{1+y}{2} + \frac{1}{129024}\big(&9c_3 M y^8\lambda + 72c_3 M y^7\lambda + 252c_3 M y^6\lambda + 504c_4 M y^5\lambda + \\
&630c_3 M y^4\lambda + 504c_3 M y^3\lambda + 252c_3 M y^2\lambda - 1080c_3 M y\lambda - 1143c_3 M\lambda - 24c_3 y^7\lambda \\
&- 168c_3 y^6\lambda - 504c_3 y^5\lambda - 840c_3 y^4\lambda - 840c_3 y^3\lambda - 504c_3 y^2\lambda + 1368c_3 y\lambda + \\
&1512c_3\lambda - 14c_4 y^9 - 126c_4 y^8 - 504c_4 y^7 - 1176c_4 y^6 - 1764c_4 y^5 - \\
&1764c_4 y^4 - 1176c_4 y^3 - 504c_4 y^2 + 3458c_4 y + 3570c_4\big).
\end{aligned} \tag{70}$$

(a) Velocity profile against parameter R using HPM solution.
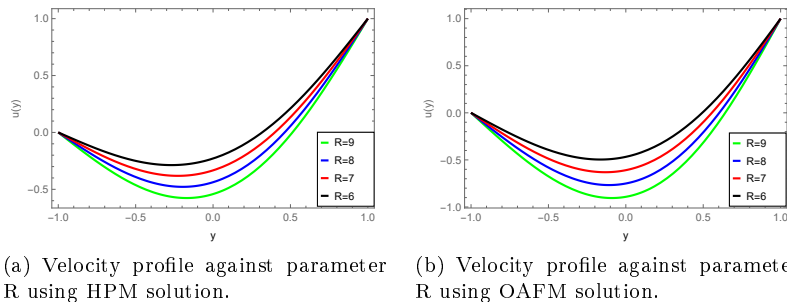
(b) Velocity profile against parameter R using OAFM solution.

Figure 2. Comparison of HPM and OAFM solutions for velocity profile against parameter R when $\lambda = 4$, $\beta = 1$ and $M = 2$.
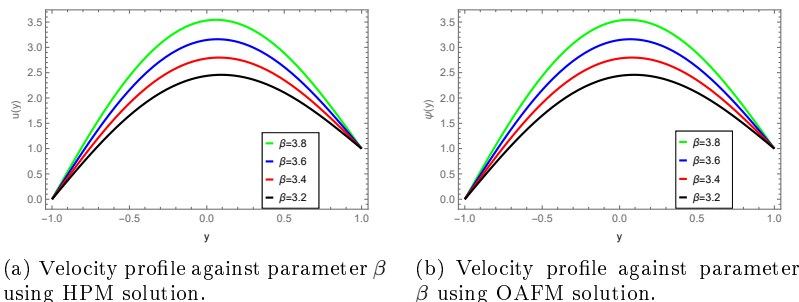

(a) Velocity profile against parameter β using HPM solution.

(b) Velocity profile against parameter β using OAFM solution.

Figure 3. Comparison of HPM and OAFM solutions for velocity profile against parameter β when $\lambda = 4$, $R = 7$ and $M = -5$.

(a) Temperature profile against parameter λ using HPM solution.

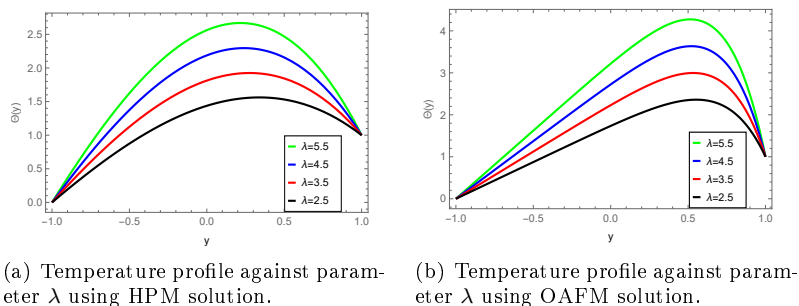(b) Temperature profile against parameter λ using OAFM solution.

Figure 6. Comparison of HPM and OAFM solutions for Temperature profile against parameter λ when R=2, $M = -4$ and $\beta = 0.4$.

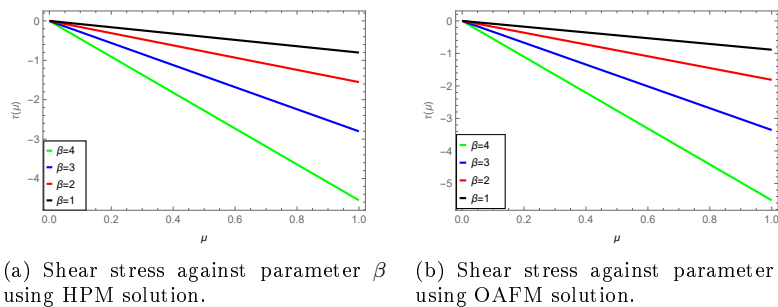(a) Shear stress against parameter β using HPM solution.

(b) Shear stress against parameter β using OAFM solution.

Figure 7. Shear stress on upper plate against parameter λ when $R = 0.3$ and $M = 3$.

(a) Velocity profile against parameter M using HPM solution.

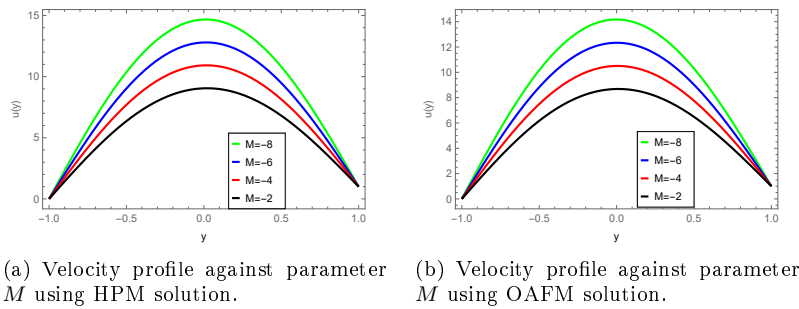(b) Velocity profile against parameter M using OAFM solution.

Figure 4. Comparison of HPM and OAFM solutions for velocity profile against parameter M when $\lambda = 4$, $R = 8$ and $\beta = 6$.

(a) Temperature profile against parameter M using HPM solution.

(b) Temperature profile against parameter M using OAFM solution.

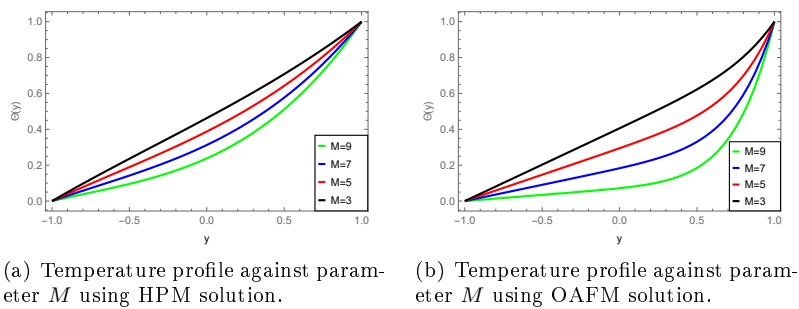**Figure 5.** Comparison of HPM and OAFM solutions for temperature distribution against parameter M when R=2, $\lambda = 0.6$ and $\beta = 0.4$.
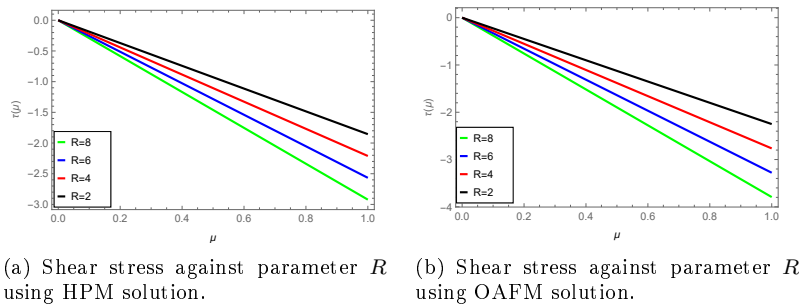

(a) Shear stress against parameter R using HPM solution.

(b) Shear stress against parameter R using OAFM solution.

Figure 8. Shear stress on upper plate against parameter R when $\beta = 2$ and $M = 3$.

(a) Shear stress against parameter β using HPM solution.

(b) Shear stress against parameter β using OAFM solution.

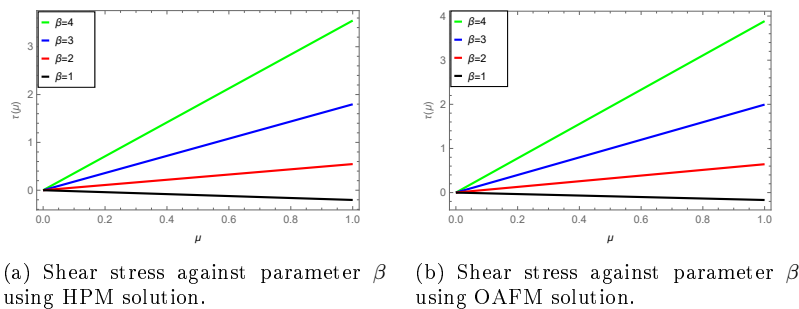**Figure 9.** Shear stress on lower plate against parameter λ when $\beta = 2$ and $R = 0.3$.

(a) Shear stress against parameter R using HPM solution.
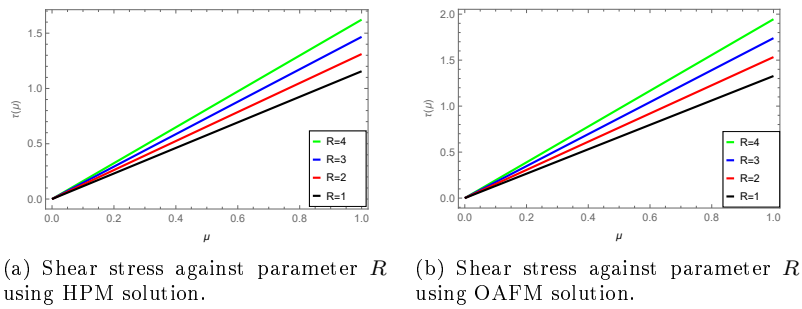
(b) Shear stress against parameter R using OAFM solution.

Figure 10. Shear stress on lower plate against parameter R when $\beta = 2$ and $M = 3$.

(a) Flow rate against parameter R using HPM solution.

(b) Flow rate against parameter R using OAFM solution.
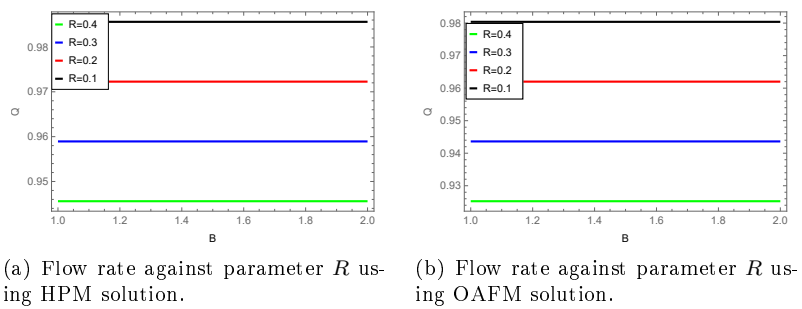
Figure 11. Flow rate against parameter R at $\beta = 2$ and $M = 3$.

(a) Flow rate against parameter M using HPM solution.

(b) Flow rate against parameter M using OAFM solution.
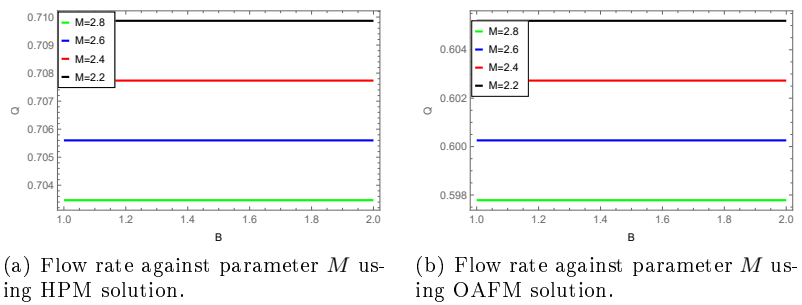
Figure 12. Flow rate against parameter M at $\beta = 2$ and $M = 3$.

NUMERICAL RESULTS AND DISCUSSION

In this paper, we utilized the homotopy perturbation method (HPM) and optimal auxiliary function method (OAFM) to investigate the couette flow of couple stress fluid under the influence of MHD. Different graphs are plotted to see the effect of various parameters on the velocity and temperature distribution. The efficiency of the proposed approaches are analyzed using different tables having the comparison of residual error obtained by OAFM and HPM. In Figure (2),the velocity profile of the fluid is plotted using both approaches and found the MHD parameter R has inverse relation with the velocity profle. Figure (3) show the comparison of HPM and OAFM for the velocity u(y) against parameter β. It reveals that β has directly relation with the velocity of fluid. Figure (4) show the inverse relation between parameter M and velocity of the fluid u(y). Figure (5) show the impact of parameter M on the temperature distributions. Figure (6) are plotted to see the effect of parameter λ on temperature distribution $\Theta(y)$ using OAFM and HPM solutions. The non-dimensional parameter λ denotes Brinkman number, which shows direct relation with the temperature distribution. Figure (7), (8) show the behaviour of shear stress **S** on the upper plate against different parameters by using HPM and OAFM solutions. Figure (9), (10) show the behaviour of shear stress **S** on the lower plate against different parameters by using HPM and OAFM solutions. Figure (11), (12) demonstrates the effect of Parameters R and M on the flow rate

using HPM and OAFM solutions. Table (1) and (2) represent the comparison of OAFM and HPM solutions and their residual error for the Velocity profile and temperature distribution. These tables compare the results obtained by both approaches for the different values of the independent variable y and parameters R, β, M, and λ. Table (3)-(6) provides skin friction for different parameter using OAFM and HPM solutions and their absolute differences. The range of residual error obtained by OAFM is -4 to -8 while the range of residual error obtained by HPM is -8 to -16. It is observed that the HPM solution is batter than OAFM solution.

Table 1. Comparison of OAFM and HPM solutions for the velocity profile keeping M=0.00015, $\lambda = 0.0001$ **and** $R = 0.00002$

y	u_{OAFM}	u_{HPM}	Residual u_{OAFM}	Residual u_{HPM}
-1.0	-2.5$\times 10^{-22}$	0	-1.6968$\times 10^{-6}$	1.47742$\times 10^{-16}$
-0.8	0.099999	0.099999	-1.3819$\times 10^{-7}$	-1.2385$\times 10^{-11}$
-0.6	0.199999	0.199999	6.2748$\times 10^{-7}$	-2.3714$\times 10^{-11}$
-0.4	0.299998	0.299998	7.4888$\times 10^{-7}$	-3.2990$\times 10^{-11}$
-0.2	0.399998	0.399998	4.1781$\times 10^{-7}$	-3.9349$\times 10^{-11}$
0.0	0.499998	0.499998	-1.0522$\times 10^{-7}$	-4.2116$\times 10^{-11}$
0.2	0.599998	0.599998	-4.9810$\times 10^{-7}$	-4.0874$\times 10^{-11}$
0.4	0.699998	0.699998	-4.5993$\times 10^{-7}$	-3.5525$\times 10^{-11}$
0.6	0.799999	0.799999	7.50698$\times 10^{-8}$	-2.6355$\times 10^{-11}$
0.8	0.899999	0.899999	5.25136$\times 10^{-7}$	-1.4098$\times 10^{-11}$
1.0	1.0000	1.0000	-1.0300$\times 10^{-6}$	-1.44731$\times 10^{-16}$

Table 2. Comparison of OAFM and HPM solutions for temperature distribution keeping R=0.00002, M=0.00015, $\beta = 0.0003$ **and** $\lambda = 0.0001$

y	Θ_{OAFM}	Θ_{HPM}	Residual Θ_{OAFM}	Residual Θ_{HPM}
-1.0	-1.7$\times 10^{-20}$	0.0000	2.5$\times 10^{-5}$	-3.1111$\times 10^{-10}$
-0.8	0.100011	0.100004	2.51$\times 10^{-5}$	1.6381$\times 10^{-9}$
-0.6	0.200023	0.200008	2.47$\times 10^{-5}$	7.0229$\times 10^{-9}$
-0.4	0.300034	0.30001	2.16$\times 10^{-5}$	1.4525$\times 10^{-8}$
-0.2	0.400045	0.400012	1.36$\times 10^{-5}$	2.2185$\times 10^{-8}$
0.0	0.500054	0.500012	3.37$\times 10^{-6}$	2.7758$\times 10^{-8}$
0.2	0.600061	0.600012	-1$\times 10^{-6}$	2.9209$\times 10^{-8}$
0.4	0.700061	0.70001	1.351$\times 10^{-6}$	2.5357$\times 10^{-8}$
0.6	0.800051	0.800008	-6.2$\times 10^{-5}$	1.6653$\times 10^{-8}$
0.8	0.900029	0.900004	6.4$\times 10^{-5}$	6.1074$\times 10^{-9}$
1.0	1.0000	1.0000	3.8$\times 10^{-4}$	3.5550$\times 10^{-10}$

Table 3. Comparison of $\Theta_{OAFM}(1)$ **and** $\Theta_{HPM}(1)$ **and their absolute difference keeping** $\beta = 0.00003$, $M = 0.000015$ **and** $R = 0.000002$.

λ	$\Theta_{OAFM}(1)$	$\Theta_{HPM}(1)$	Abs.difference
0	0.500825	0.5	8.25$\times 10^{-4}$
0.000015	0.500681	0.499996	6.8$\times 10^{-4}$
0.00003	0.500537	0.499993	5.45$\times 10^{-4}$
0.000045	0.500394	0.499989	4.05$\times 10^{-4}$
0.00006	0.50025	0.499985	2.65$\times 10^{-4}$
0.000075	0.500106	0.499981	1.25$\times 10^{-4}$
0.00009	0.499962	0.499978	1.51$\times 10^{-4}$
0.000105	0.499819	0.499974	1.55$\times 10^{-4}$
0.00012	0.499675	0.49997	2.95$\times 10^{-4}$
0.000135	0.499531	0.499966	4.35$\times 10^{-4}$
0.00015	0.499387	0.499963	5.75$\times 10^{-4}$

Table 4. Comparison of $\Theta_{OAFM}(-1)$ and $\Theta_{HPM}(-1)$ and their absolute difference keeping
$\beta = 0.00003$, $M = 0.000015$ and $R = 0.000002$.

λ	$\Theta_{OAFM}(-1)$	$\Theta_{HPM}(-1)$	Abs.difference
0.000	0.499897	0.5000	1.03×10^{-4}
0.000015	0.499921	0.500004	8.29×10^{-5}
0.00003	0.499945	0.500007	6.27×10^{-5}
0.000045	0.499969	0.500011	4.25×10^{-5}
0.00006	0.499993	0.500015	2.23×10^{-5}
0.000075	0.500017	0.500019	2.07×10^{-6}
0.00009	0.500041	0.500022	1.81×10^{-5}
0.000105	0.500065	0.500026	3.83×10^{-5}
0.00012	0.500089	0.50003	5.85×10^{-5}
0.000135	0.500112	0.500034	7.87×10^{-5}
0.00015	0.500136	0.500037	9.90×10^{-5}

Table 5. Comparison of $\Theta_{OAFM}(1)$ and $\Theta_{HPM}(1)$ and their absolute difference keeping
$\beta = 0.00003$, $\lambda = 0.000015$ and $R = 0.000002$.

M	$\Theta_{OAFM}(1)$	$\Theta_{HPM}(1)$	Abs.difference
0	0.500681	0.499996	6.85×10^{-4}
0.000025	0.500681	0.499996	6.85×10^{-4}
0.00005	0.500681	0.499996	6.85×10^{-4}
0.000075	0.500681	0.499996	6.85×10^{-4}
0.0001	0.500681	0.499996	6.85×10^{-4}
0.000125	0.500681	0.499996	6.85×10^{-4}
0.00015	0.500681	0.499996	6.85×10^{-4}
0.000175	0.500681	0.499996	6.85×10^{-4}
0.0002	0.500681	0.499996	6.85×10^{-4}
0.000225	0.500681	0.499996	6.85×10^{-4}
0.00025	0.500681	0.499996	6.85×10^{-4}

Table 6. Comparison of $\Theta_{OAFM}(-1)$ and $\Theta_{HPM}(-1)$ and their absolute difference keeping
$\beta = 0.00003$, $\lambda = 0.000015$ and $R = 0.000002$.

M	$\Theta_{OAFM}(-1)$	$\Theta_{HPM}(-1)$	Abs.difference
0	0.499921	0.500004	8.29×10^{-5}
0.000015	0.499921	0.500004	8.29×10^{-5}
0.00003	0.499921	0.500004	8.29×10^{-5}
0.000045	0.499921	0.500004	8.29×10^{-5}
0.00006	0.499921	0.500004	8.29×10^{-5}
0.000075	0.499921	0.500004	8.29×10^{-5}
0.00009	0.499921	0.500004	8.29×10^{-5}
0.000105	0.499921	0.500004	8.29×10^{-5}
0.00012	0.499921	0.500004	8.29×10^{-5}
0.000135	0.499921	0.500004	8.29×10^{-5}
0.00015	0.499921	0.500004	8.29×10^{-5}

CONCLUSIONS

In this paper, plane couette flow of a couple stress fluid under the influence of magnetohydrodynamics (MHD) using Reynolds model of viscosity has been explored by employing two reliable techniques. The governing equation of the couple stress fluid under the influence of MHD are solved using Homotpoy Perturbation method (HPM) and Optimal Auxiliary Function Method (OAFM). The HPM is an analytical method that employs a

series solution with a parameter to approximate the solution of the problem. On the other hand, the OAFM is a numerical technique that involves introducing an auxiliary function to simplify the equations, leading to an easier solution procedure and gives an efficient solution after two steps. Furthermore the effect of non-dimensional parameters on velocity profile, temperature distribution, shear stresses and flow rate are analysed. The HPM solution and OAFM solution are compared to each other using different graphs and tables involving residual error. It reveals that the HPM solution is more efficient and accurate than OAFM solution. Finally we conclude that both approaches have the capability to solve highly non linear differential equations and physical models.

Conflicts of Interest

The authors declare that there are no conflicts of interest regarding the publication of this article.

Acknowledgments

ORCID

Muhammad Farooq, https://orcid.org/0000-0003-3392-101X; Ibrar Khan, https://orcid.org/0009-0008-2586-9841; Rashid Nawaz, https://orcid.org/0000-0002-4773-8446; Gamal M. Ismail, https://orcid.org/0000-0002-9060-4371; Huzaifa Umar, https://orcid.org/0000-0003-2508-9710; Hijaz Ahmad, https://orcid.org/0000-0002-5438-5407

REFERENCES

[1] M.A. Seddeek, "Heat and mass transfer on a stretching sheet with a magnetic field in a visco-elastic fluid flow through a porous medium with heat source or sink," Computational Materials Science, **38**(4), 781-787 (2007). https://doi.org/10.1016/j.commatsci.2006.05.015

[2] M.A. Mansour, M.A. El-Hakiem, and S.M. El Kabeir, "Heat and mass transfer in magnetohydrodynamic flow of micropolar fluid on a circular cylinder with uniform heat and mass flux," Journal of Magnetism and Magnetic Materials, **220**(2-3), 259-270 (2000). https://doi.org/10.1016/S0304-8853(00)00488-1

[3] O.A. Bég, A.Y. Bakier, V.R. Prasad, J. Zueco, and S.K. Ghosh, "Nonsimilar, laminar, steady, electrically-conducting forced convection liquid metal boundary layer flow with induced magnetic field effects," International Journal of Thermal Sciences, **48**(8), 1596-1606 (2009). https://doi.org/10.1016/j.ijthermalsci.2008.12.007

[4] R. Jain, R. Mehta, M.K. Sharma, T. Mehta, H. Ahmad, and F. Tchier, "Numerical analysis of heat and mass transport of hybrid nanofluid over an extending plate with inclined magnetic field in presence of Soret and dufour Effect," Modern Physics Letters B, **6**, 2450037 (2023). https://doi.org/10.1142/S0217984924500374

[5] S.F. Megahid, A.E. Abouelregal, H. Ahmad, M.A. Fahmy, and H. Abu-Zinadah, "A generalized More-Gibson-Thomson heat transfer model for the study of thermomagnetic responses in a solid half-space," Results in Physics, **51**, 106619 (2023). https://doi.org/10.1016/j.rinp.2023.106619

[6] T. Muhammad, H. Ahmad, U. Farooq, and A. Akgül, "Computational Investigation of Magnetohydrodynamics Boundary of Maxwell Fluid Across Nanoparticle-Filled Sheet," Al-Salam Journal for Engineering and Technology, **2**(2), 88-97 (2023). https://doi.org/10.55145/ajest.2023.02.02.011

[7] A.E. Abouelregal, H. Ahmad, M.A. Aldahlan, and X.Z. Zhang, "Nonlocal magneto-thermoelastic infinite half-space due to a periodically varying heat flow under Caputo–Fabrizio fractional derivative heat equation," Open Physics, **20**(1), 274-288 (2022). https://doi.org/10.1515/phys-2022-0019

[8] M. Farooq, Z. Ahmad, H. Ahmad, M. Zeb, F. Aouaini, and M. Ayaz, "Homotopy analysis methods with applications to thin-film flow of a magnetohydrodynamic-modified second grade fluid," Modern Physics Letters B, **36**(19), 2150617 (2022). https://doi.org/10.1142/S021798492150617X

[9] H. Ahmad, A.E. Abouelregal, M. Benhamed, M.F. Alotaibi, and A. Jendoubi, "Vibration analysis of nanobeams subjected to gradient-type heating due to a static magnetic field under the theory of nonlocal elasticity," Scientific Reports, **12**(1), 1894 (2022). https://doi.org/10.1038/s41598-022-05934-0

[10] B. Tashtoush, "Magnetic and buoyancy effects on melting from a vertical plate embedded in saturated porous media," Energy Conversion and Management, **46**(15-16), 2566-2577 (2005). https://doi.org/10.1016/j.enconman.2004.12.004

[11] M.F. El-Amin, "Magnetohydrodynamic free convection and mass transfer flow in micropolar fluid with constant suction," Journal of magnetism and magnetic materials, **234**(3), 567-574 (2001). https://doi.org/10.1016/S0304-8853(01)00374-2

[12] S. Ahmed, O.A. Bég, and S.K. Ghosh, "A couple stress fluid modeling on free convection oscillatory hydromagnetic flow in an inclined rotating channel," Ain Shams Engineering Journal, **5**(4), 1249-1265 (2014). https://doi.org/10.1016/j.asej.2014.04.006

[13] A.A. Dar, and K. Elangovan, "Influence of an inclined magnetic field on Heat and Mass transfer of the peristaltic flow of a couple stress fluid in an inclined channel," World Journal of Engineering, **14**(1), 7-18 (2017). https://doi.org/10.1108/WJE-11-2016-0124

[14] P.Y. Xiong, M. Nazeer, F. Hussain, M.I. Khan, A. Saleem, S. Qayyum, and Y.M. Chu, "Two-phase flow of couple stress fluid thermally effected slip boundary conditions: Numerical analysis with variable liquids properties," Alexandria Engineering Journal, **61**(5), 3821-3830 (2022). https://doi.org/10.1016/j.aej.2021.09.012

[15] O.A. Ajala, L.O. Aselebe, S.F. Abimbade, and A.W. Ogunsola, "Effect of magnetic fields on the boundary layer flow of heat transfer with variable viscosity in the presence of thermal radiation," International Journal of Scientific and Research Publication, **9**(5), 13-19 (2019). https://doi.org/10.24297/jam.v12i7.3874

[16] J.A. Falade, S.O. Adesanya, J.C. Ukaegbu, and M.O. Osinowo, "Entropy generation analysis for variable viscous couple stress fluid flow through a channel with non-uniform wall temperature," Alexandria Engineering Journal, **55**(1), 69-75 (2016). https://doi.org/10.1016/j.aej.2016.01.011

[17] B.V. Swarnalathamma, and M.V. Krishna, "Peristaltic hemodynamic flow of couple stress fluid through a porous medium under the influence of magnetic field with slip effect," In AIP Conference Proceedings, **1728**(1), 020603 (2016). https://doi.org/10.1063/1.4946654

[18] K. Ramesh, "Influence of heat and mass transfer on peristaltic flow of a couple stress fluid through porous medium in the presence of inclined magnetic field in an inclined asymmetric channel," Journal of Molecular Liquids, **219**, 256-271 (2016). https://doi.org/10.1016/j.molliq.2016.03.010

[19] B.B. Divya, G. Manjunatha, C. Rajashekhar, H. Vaidya, and K.V. Prasad, "Effects of inclined magnetic field and porous medium on peristaltic flow of a Bingham fluid with heat transfer," Journal of Applied and Computational Mechanics, **7**(4), 1892-1906 (2021). https://doi.org/10.22055/JACM.2019.31060.1822

[20] T. Hayat, M. Awais, A. Safdar, and A.A. Hendi, "Unsteady three dimensional flow of couple stress fluid over a stretching surface with chemical reaction," Nonlinear Analysis: Modelling and Control, **17**(1), 47-59 (2012). https://doi.org/10.15388/NA.17.1.14077

[21] S.T. Mohyud-Din, and M.A. Noor, "Homotopy perturbation method for solving partial differential equations," Zeitschrift für Naturforschung A, **64**(3-4), 157-170 (2009). https://doi.org/10.1515/zna-2009-3-402

[22] J. Biazar, and H. Ghazvini, "Convergence of the homotopy perturbation method for partial differential equations," Nonlinear Analysis: Real World Applications, **10**(5), 2633-2640 (2009). https://doi.org/10.1016/j.nonrwa.2008.07.002

[23] B. Marinca, and V. Marinca, "Approximate analytical solutions for thin film flow of a fourth grade fluid down a vertical cylinder," Proceed Romanian Academy, Series A, **19**(1), 69-76 (2018). https://acad.ro/sectii2002/proceedings/doc2018-1/10.pdf

[24] L. Zada, R. Nawaz, M. Ayaz, H. Ahmad, H. Alrabaiah, and Y.M. Chu, "New algorithm for the approximate solution of generalized seventh order Korteweg-Devries equation arising in shallow water waves," Results in Physics, **20**, 103744 (2021). https://doi.org/10.1016/j.rinp.2020.103744

[25] S. Islam, and C.Y. Zhou, "Exact solutions for two dimensional flows of couple stress fluids," Zeitschrift für angewandte Mathematik und Physik, **58**(6), 1035-1048 (2007). https://doi.org/10.1007/s00033-007-5075-5

[26] N.T. EL-Dabe, and S.M. El-Mohandis, "Effect of couple stresses on pulsatile hydromagnetic Poiseuille flow," Fluid Dynamics Research, **15**(5), 313-324 (1995). https://doi.org/10.1016/0169-5983(94)00049-6

[27] Y. Aksoy, and M. Pakdemirli, "Approximate analytical solutions for flow of a third-grade fluid through a parallel-plate channel filled with a porous medium," Transport in Porous Media, **83**, 375-395 (2010). https://doi.org/10.1007/s11242-009-9447-5

[28] M. Massoudi, and I. Christie, "Effects of variable viscosity and viscous dissipation on the flow of a third grade fluid in a pipe," International Journal of Non-Linear Mechanics, **30**(5), 687-699 (1995). https://doi.org/10.1016/0020-7462(95)00031-I

[29] T. Chinyoka, and O.D. Makinde, "Analysis of transient Generalized Couette flow of a reactive variable viscosity third-grade liquid with asymmetric convective cooling," Mathematical and Computer Modelling, **54**(1-2), 160-174 (2011). http://dx.doi.org/10.1016/j.mcm.2011.01.047

ПОРІВНЯЛЬНИЙ АНАЛІЗ ПЛОСКОЇ ТЕЧІЇ КУЕТТА ПАРНО НАПРУЖЕНОЇ РІДИНИ ПІД ВПЛИВОМ МАГНІТОГІДРОДИНАМІКИ

Мухаммад Фарук[a]**, Ібрар Хан**[a]**, Рашид Наваз**[b]**, Гамаль Мохамед Ісмаїл**[c]**, Хузайфа Умар**[d]**, Хіджаз Ахмад**[c,d,e]

[a] *Факультет математики, Університет Абдула Валі Хана, Мардан 23200, Пакистан*
[b] *UniSa STEM, Університет Південної Австралії*
[c] *Департамент математики, Факультет природничих наук, Ісламський університет Медіни, Медіна, Саудівська Аравія*
[d] *Близькосхідний університет, Центр оперативних досліджень у сфері охорони здоров'я, Близькосхідний бульвар, ПК: 99138 Нікосія/Мерсін 10, Туреччина*
[e] *Департамент математики, Азербайджанський університет, вул. Джейхун Гаджибейлі, 71, AZ1007, Баку, Азербайджан*

Це дослідження має на меті виконати порівняльний аналіз плоского потоку Куетта парної напруженої рідини під впливом магнітогідродинаміки (МГД) за допомогою двох різних методів: методу оптимальної допоміжної функції (OAFM) і методу гомотопічних збурень (HPM). Рідина парних напружень відома своєю неньютонівською поведінкою, де реакція рідини на зсув залежить від наявності внутрішньої мікроструктури. OAFM і HPM використовуються для розв'язання керівних рівнянь течії рідини парних напруг під МГД. OAFM — це чисельний метод, який передбачає введення допоміжної функції для спрощення рівнянь, що спрощує процедуру розв'язання. З іншого боку, HPM — це аналітичний метод, який використовує послідовне рішення. Порівняльний аналіз зосереджується на вивченні точності, ефективності та поведінки збіжності двох методів. Для дослідження їх впливу на поведінку потоку розглядаються різні параметри потоку, такі як параметр напруги пари, магнітний параметр і співвідношення швидкостей. Крім того, рішення HPM порівнювали з рішенням OAFM за допомогою різних графіків і таблиць. Це виявило, що рішення, отримане HPM, є кращим, ніж рішення OAFM.

Ключові слова: *парно напружена рідина; метод оптимальної допоміжної функції (OAFM); метод гомотопічних збурень (HPM); магнітогідродинаміка (MHD)*